PROCEEDINGS OF SCIENCE

Search for new physics in semileptonic B-decays

Suzanne Klaver[*†]
The University of Manchester, Manchester, UK
E-mail: suzanne.klaver@cern.ch

Semileptonic decays provide an excellent environment for testing the Standard Model (SM). Violation of lepton universality would be a smoking gun for physics beyond the SM. Using semitauonic B decays, LHCb finds a value of $\mathscr{R}(D^*) = \mathscr{B}(\bar{B}^0 \to D^{*+}\tau^-\overline{\nu}_\tau)/\mathscr{B}(\bar{B}^0 \to D^{*+}\mu^-\overline{\nu}_\mu) = 0.336 \pm 0.027(\text{stat}) \pm 0.030(\text{syst})$, which is 2.1 standard deviations larger than the value expected from the SM. Moreover, the measurement of the *CP* asymmetry in mixing of B_s^0 mesons is highly sensitive to physics beyond the SM. This article presents the latest result on semileptonic asymmetries; using the full Run 1 dataset, it is found that $a_{\text{sl}}^s = (0.39 \pm 0.26(\text{stat}) \pm 0.20(\text{syst}))\%$, which is consistent with the Standard Model.

38th International Conference on High Energy Physics
3-10 August 2016
Chicago, USA

[*]Speaker.
[†]On behalf of the LHCb collaboration

© Copyright owned by the author(s) under the terms of the Creative Commons Attribution-NonCommercial-NoDerivatives 4.0 International License (CC BY-NC-ND 4.0).

arXiv:1611.08250v1 [hep-ex] 24 Nov 2016

1. Introduction to semileptonic B-decays

Semileptonic decays are abundant and provide an excellent environment for precision physics as they can be precisely predicted theoretically. The outstanding vertex resolution of the LHCb detector [1, 2] enables to carry out many exciting analyses involving semileptonic B decays. This article summarises two results from LHCb: a test of lepton universality in $\mathscr{R}(D^*)$ and the measurement of CP violation in B_s^0-$\bar{B}_s^0$ mixing, both of which use the $3.0\,\text{fb}^{-1}$ dataset recorded in 2011 and 2012.

2. Testing lepton universality in $\mathscr{R}(D^*)$

In the Standard Model, the branching fractions $\mathscr{B}(\bar{B}^0 \to D^{*+}\tau^-\overline{\nu}_\tau)$ and $\mathscr{B}(\bar{B}^0 \to D^{*+}\mu^-\overline{\nu}_\mu)$ differ only due to the difference in lepton mass between the two decays. However, in many extensions of the SM, enhanced couplings to the third generation are predicted, in particular models containing charged Higgs bosons. The measurement of the ratio of branching fractions:

$$\mathscr{R}(D^*) \equiv \frac{\mathscr{B}(\bar{B}^0 \to D^{*+}\tau^-\overline{\nu}_\tau)}{\mathscr{B}(\bar{B}^0 \to D^{*+}\mu^-\overline{\nu}_\mu)}, \tag{2.1}$$

therefore tests this idea of lepton universality present in the SM, which predicts a value of $\mathscr{R}(D^*) = 0.252 \pm 0.003$ [3].

The τ^- candidate is reconstructed as $\tau^- \to \mu^-\overline{\nu}_\mu\nu_\tau$, hence the signal channel has the same visible final-state as the control channel $\bar{B}^0 \to D^{*+}\mu^-\overline{\nu}_\mu$ [4]. The selection for both decays is similar which combines a muon and the D^{*+} candidate that is reconstructed through $D^{*+} \to D^0(\to K^-\pi^+)\pi^+$. In addition to the signal and normalisation channel, also several background processes are selected, which are suppressed by exploiting kinematic and topological properties.

A multidimensional fit is performed to measure to signal, normalisation and background components. The variables used for the fit are kinematic variables which are most discriminating between the signal and normalisation channel. These are the missing mass squared, m^2_{miss}, the muon energy in the center-of-mass, E^*_μ, and the squared four-momentum of the lepton system, q^2. Simulated distributions of the signal and normalisation channel of these variables are shown in Fig. 1.

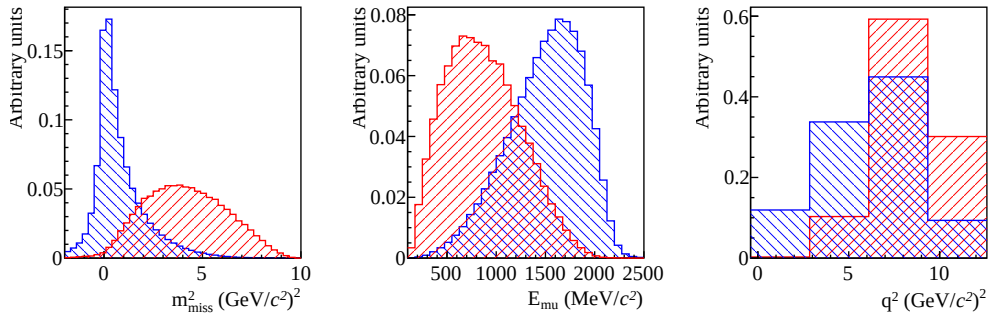

Figure 1: Simulated distributions of the kinematic variables that are used in the fits. In blue are the distributions from the normalisation channel: $\bar{B}^0 \to D^{*+}\mu^-\overline{\nu}_\mu$, and in red from the signal: $\bar{B}^0 \to D^{*+}\tau^-\overline{\nu}_\tau$. From left to right are the distributions of m^2_{miss}, E^*_μ, and q^2.

The three-dimensional fit is performed using templates of the signal, normalisation, and background channels. Projections in m^2_{miss} and E^*_μ of the data and fits in the two highest bins of q^2 are shown in Fig. 2. The shapes from the combinatorial and misidentified backgrounds are taken from data, while the physics background are modelled using control samples. The $\bar{B}^0 \to D^{*+}\tau^-\bar{\nu}_\tau$ is most visible in the highest q^2 bin.

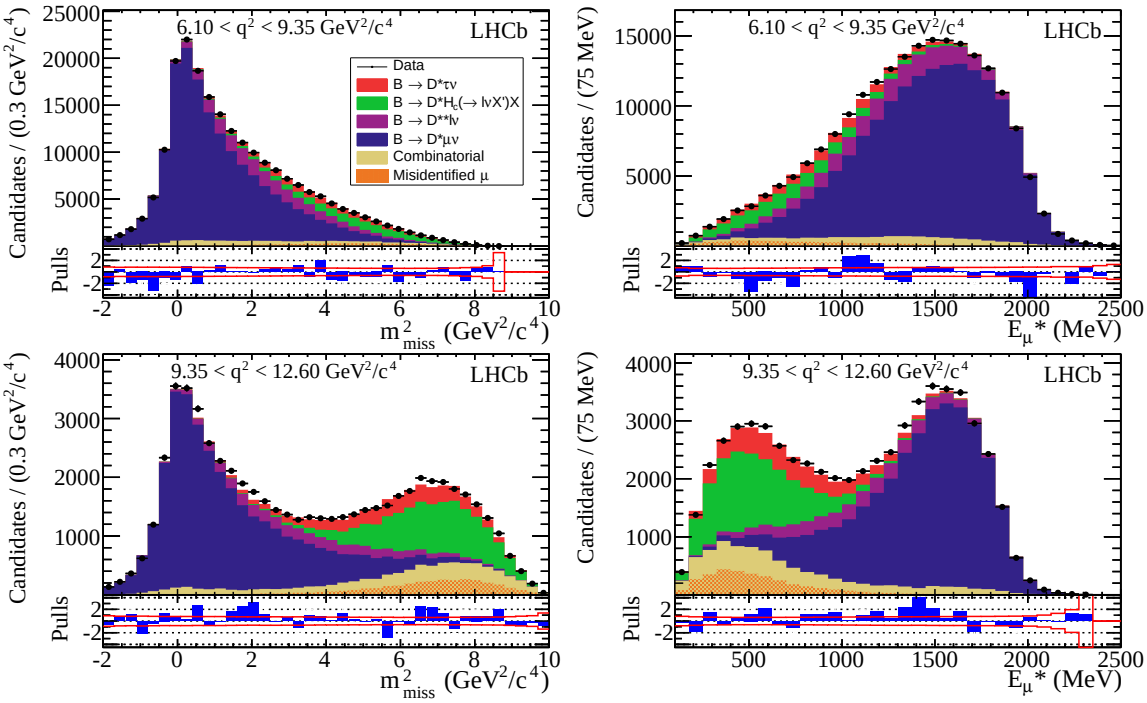

Figure 2: Distributions of m^2_{miss} (left) and E^*_μ (right) in the two highest q^2 bins of the signal data, overlaid with the projections of the fit model. The signal distributions are red, and the normalisation channel is blue.

The LHCb measurement is $\mathscr{R}(D^*) = 0.336 \pm 0.027(\text{stat}) \pm 0.030(\text{syst})$, which is the first measurement of a B to τ decay at a hadron collider. Fig. 3 (left) shows the LHCb measurement of $\mathscr{R}(D^*)$ and those performed by Belle [5, 6, 7] and BaBar [8], which indicates consistency between the experimental results. Fig. 3 (right) displays the $\mathscr{R}(D)$ vs. $\mathscr{R}(D^*)$ measurements and the current theoretical predictions, indicating a 3.9σ discrepancy between theory and experiment. This could be explained by *e.g.* models containing an additional charged Higgs [9].

3. Measuring *CP* violation in B^0_s-$\bar{B}^0_s$ mixing

Neutral mesons can oscillate into their own antiparticle through a second-order weak amplitude in a process called mixing. Since these processes are heavily suppressed in the Standard Model, they are sensitive to new physics. This analysis concerns the measurement of the *CP* violation in mixing of B^0_s mesons, which occurs when $\mathscr{P}(B^0_s \to \bar{B}^0_s) \neq \mathscr{P}(\bar{B}^0_s \to B^0_s)$. The amount of *CP* violation in mixing can be measured using flavour-specific decays, of which the final state f indicates whether the B decayed as a B^0_s or $\bar{B}^0_s$. The flavour-specific asymmetry, a_{fs}, is defined as:

$$a_{\text{fs}} = \frac{\Gamma(\bar{B}_q \to B_q \to f) - \Gamma(B_q \to \bar{B}_q \to \bar{f})}{\Gamma(\bar{B}_q \to B_q \to f) + \Gamma(B_q \to \bar{B}_q \to \bar{f})}. \tag{3.1}$$

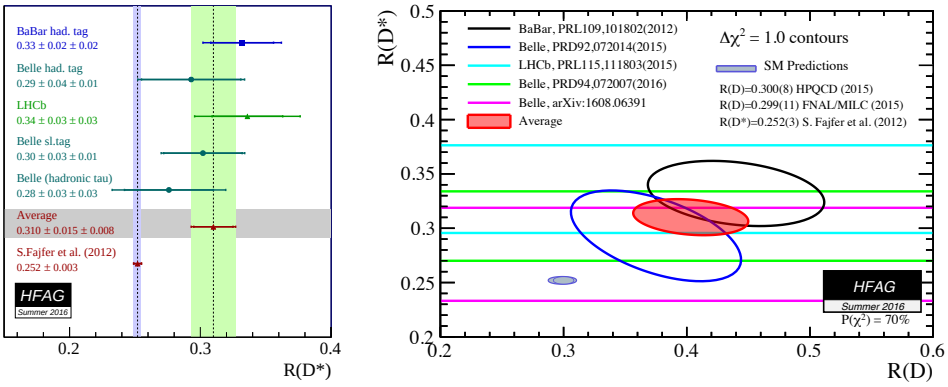

Figure 3: On the left: comparisons of the LHCb $\mathscr{R}(D^*)$ result with those from Belle [5, 6, 7] and BaBar [8]. On the right: the comparison of the LHCb measurement of $\mathscr{R}(D^*)$ with the $\mathscr{R}(D)$ vs. $\mathscr{R}(D^*)$ measurements of BaBar and Belle and the Standard Model predictions [3, 10, 11] from HFAG [12].

For the B_s^0 mesons, this quantity is called $a_{\rm sl}^s$, and for the B^0 system, $a_{\rm sl}^d$. The Standard Model predictions for both are very small: $a_{\rm sl}^s = (2.22 \pm 0.27) \times 10^{-5}$ and $a_{\rm sl}^d = (-4.7 \pm 0.6) \times 10^{-4}$ [13]. In their dimuon measurement, D0 has found a discrepancy of a combination of $a_{\rm sl}^s$ and $a_{\rm sl}^d$ with respect to the SM value of 3σ [14].

To measure $a_{\rm sl}^s$ in LHCb, the inclusive semileptonic decay $B_s^0 \to D_s^- \mu^+ \nu_\mu$ is studied, where the D_s^- is reconstructed in the $K^+K^-\pi^\mp$ final state. The full phase space of the D_s^- decay is analysed, divided into three regions of the Dalitz plane: the $\phi\pi$ region, where the K^+K^- pair goes through the ϕ resonance; the K^*K region, where the $K^+\pi^-$ pair goes through the $K^*(892)^0$ resonance; and the non-resonant region, NR. These regions are indicated in Fig. 4 (left). Backgrounds from partially reconstructed and misidentified decays are removed, as well as the backgrounds coming from B_s^0 from D decays. The signal yields are obtained by matching $D_s^-\mu^+$ pairs and fitting the D_s^- yields, which are shown in Fig. 4 (right).

The asymmetry in the signal yields is the raw asymmetry, $A_{\rm raw}$, which is defined as:

$$A_{\rm raw} = \frac{N(D_s^-\mu^+) - N(D_s^+\mu^-)}{N(D_s^-\mu^+) + N(D_s^+\mu^-)}. \tag{3.2}$$

To measure $a_{\rm sl}^s$, this asymmetry needs to be corrected for the detection asymmetries, $A_{\rm det}$, and the asymmetries from peaking backgrounds. These are the production asymmetries from B decays that peak in the D_s^- mass and called $A_{\rm bkg}$, while the fraction of these backgrounds is $f_{\rm bkg}$. $a_{\rm sl}^s$ can then be determined as follows:

$$a_{\rm sl}^s = \frac{2}{1 - f_{\rm bkg}} (A_{\rm raw} - A_{\rm det} - f_{\rm bkg} A_{\rm bkg}). \tag{3.3}$$

The detection asymmetries arise from a difference in reconstruction efficiency between positively and negatively charged particles, and can be split in tracking, trigger and particle identification asymmetries. All of those are measured using data-driven methods. As the largest systematic in the previous measurement of $a_{\rm sl}^s$ was that of the tracking asymmetry, the current analysis uses two different methods to determine these and the combination of these two is shown as a function of π momentum in Fig. 5 (left).

The latest LHCb measurement of $a^s_{\rm sl}$ uses the full 3.0 fb^{-1} of the Run 1 dataset and measures $a^s_{\rm sl} = (0.39 \pm 0.26 \pm 0.20)\%$, where the first uncertainty is statistical and the second systematic [15]. The result shown in the overview plot in Fig. 5 together with the measurements of $a^s_{\rm sl}$ and $a^d_{\rm sl}$ from D0 [16, 17], BaBar [18, 19] and Belle [20]. It is consistent with the Standard Model prediction and does not confirm the discrepancy arising from the D0 dimuon analysis [14].

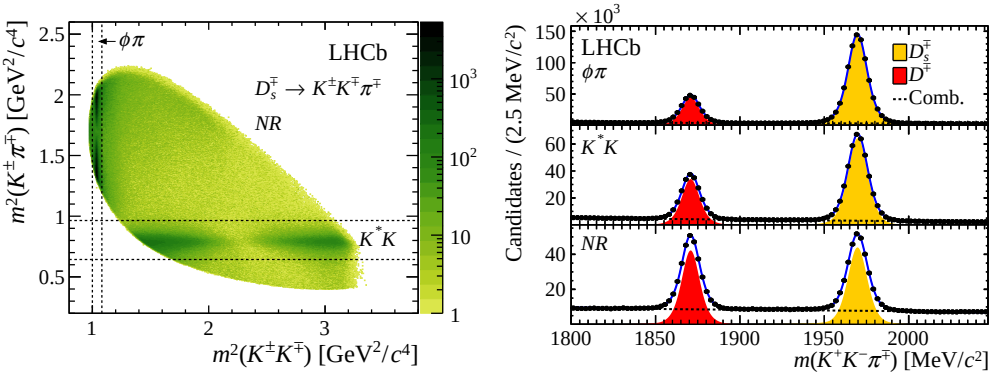

Figure 4: On the left: the Dalitz plot of the $D_s^\mp \to K^\pm K^\mp \pi^\mp$ decay for the selected $D_s^\mp\ \mu^\pm$ candidates, showing the three regions. On the right: the mass distributions of the $K^+K^-\pi^\mp$ mass for the three Dalitz regions, overlaid with the results of the signal and combinatorial fit.

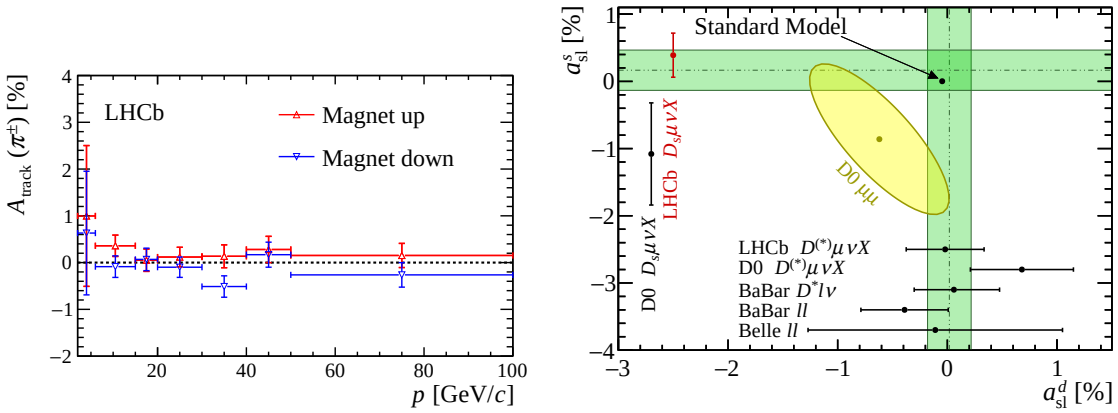

Figure 5: On the left: the π tracking asymmetry as a function of momentum. On the right: overview of the current $a^s_{\rm sl}$ and $a^d_{\rm sl}$ measurements. The yellow ellipse shows the result of the D0 dimuon measurement [14], while the points with error bars show the individual measurement of $a^s_{\rm sl}$ or $a^d_{\rm sl}$ from LHCb [15, 21], BaBar [18, 19], Belle [20], and D0 [16, 17]. The green bands are the averages of $a^s_{\rm sl}$ and $a^d_{\rm sl}$.

4. Conclusion

This article presents two semileptonic measurements from the LHCb collaboration. The $\mathcal{R}(D^*)$ measurement provides a test of lepton universality and measures a value of $\mathcal{R}(D^*) = 0.336 \pm 0.027(\text{stat}) \pm 0.030(\text{syst})$, which is 2.1σ larger than the value expected from the Standard Model. The $a^s_{\rm sl}$ analysis measures *CP* violation in mixing of B^0_s-$\bar{B}^0_s$ mesons and finds that $a^s_{\rm sl} = (0.39 \pm 0.26(\text{stat}) \pm 0.20(\text{syst}))\%$, which is the most precise measurement of *CP* violation in the B^0_s system to date and is consistent with the SM value.

References

[1] A. A. Alves Jr. et al. The LHCb detector at the LHC. *JINST*, 3:S08005, 2008.

[2] R. Aaij et al. LHCb detector performance. *Int. J. Mod. Phys.*, A30:1530022, 2015.

[3] S. Fajfer, J.F. Kamenik, and I. Nisandzic. On the $B \to D^* \tau \bar{\nu}_\tau$ Sensitivity to New Physics. *Phys. Rev.*, D85:094025, 2012.

[4] R. Aaij et al. Measurement of the ratio of branching fractions $\mathscr{B}(\overline{B}^0 \to D^{*+}\tau^-\overline{\nu}_\tau)/\mathscr{B}(\overline{B}^0 \to D^{*+}\mu^-\overline{\nu}_\mu)$. *Phys. Rev. Lett.*, 115:111803, 2015.

[5] A. Bozek et al. Observation of $B^+ \to \bar{D}^{*0}\tau^+\nu_\tau$ and Evidence for $B^+ \to \bar{D}^0\tau^+\nu_\tau$ at Belle. *Phys. Rev.*, D82:072005, 2010.

[6] M. Huschle et al. Measurement of the branching ratio of $\bar{B} \to D^{(*)}\tau^-\bar{\nu}_\tau$ relative to $\bar{B} \to D^{(*)}\ell^-\bar{\nu}_\ell$ decays with hadronic tagging at Belle. *Phys. Rev.*, D92(7):072014, 2015.

[7] A. Abdesselam et al. Measurement of the branching ratio of $\bar{B}^0 \to D^{*+}\tau^-\bar{\nu}_\tau$ relative to $\bar{B}^0 \to D^{*+}\ell^-\bar{\nu}_\ell$ decays with a semileptonic tagging method. 2016.

[8] J.P. Lees et al. Evidence for an excess of $\bar{B} \to D^{(*)}\tau^-\bar{\nu}_\tau$ decays. *Phys. Rev. Lett.*, 109:101802, 2012.

[9] A. Crivellin, J. Heeck, and P. Stoffer. A perturbed lepton-specific two-Higgs-doublet model facing experimental hints for physics beyond the Standard Model. *Phys. Rev. Lett.*, 116(8):081801, 2016.

[10] H. Na, C.M. Bouchard, G.P. Lepage, C. Monahan, and J. Shigemitsu. $B \to Dl\nu$ form factors at nonzero recoil and extraction of $|V_{cb}|$. *Phys. Rev.*, D92(5):054510, 2015. [Erratum: Phys. Rev.D93, no.11, 119906(2016)].

[11] J.A. Bailey et al. $B \to$ D łν form factors at nonzero recoil and $|V_{cb}|$ from 2+1-flavor lattice QCD. *Phys. Rev.*, D92(3):034506, 2015.

[12] Y. Amhis et al. Averages of b-hadron, c-hadron, and τ-lepton properties as of summer 2014. 2014. Link to plot.

[13] M. Artuso, G. Borissov, and A. Lenz. CP Violation in the B_s^0 System. 2015.

[14] V.M. Abazov et al. Study of *CP*-violating charge asymmetries of single muons and like-sign dimuons in $p\overline{p}$ collisions. *Phys.Rev.*, D89:012002, 2014.

[15] R. Aaij et al. Measurement of the *CP* asymmetry in $B_s^0 - \overline{B}_s^0$ mixing. *Phys. Rev. Lett.*, 117:061803, 2016.

[16] V.M. Abazov et al. Measurement of the semileptonic charge asymmetry in B^0 meson mixing with the D0 detector. *Phys.Rev.*, D86:072009, 2012.

[17] V.M. Abazov et al. Measurement of the semileptonic charge asymmetry using $B_s^0 \to D_s\mu X$ decays. *Phys.Rev.Lett.*, 110:011801, 2013.

[18] J. P. Lees et al. Search for *CP* violation in B^0-$\bar{B}^0$ mixing using partial reconstruction of $B^0 \to D^{*-}X\ell^+\nu_\ell$ and a kaon tag. *Phys.Rev.Lett.*, 111:101802, 2013.

[19] J. P. Lees et al. Study of *CP* Asymmetry in $B^0 - \bar{B}^0$ Mixing with Inclusive Dilepton Events. *Phys. Rev. Lett.*, 114(8):081801, 2015.

[20] E. Nakano et al. Charge asymmetry of same-sign dileptons in B^0-$\bar{B}^0$ mixing. *Phys.Rev.*, D73:112002, 2006.

[21] R. Aaij et al. Measurement of the semileptonic *CP* asymmetry in B^0–$\overline{B}^0$ mixing. *Phys. Rev. Lett.*, 114: 041601, 2015.